

The InAs Electron Avalanche Photodiode

Dr. Andrew R. J. Marshall
Lancaster University
England

1. Introduction

Avalanche photodiodes (APDs) exploit the process of impact ionisation to amplify the primary, or unity gain, photocurrent generated by the absorption of incident photons. In all APDs the signal enhancing avalanche multiplication is accompanied by an increase in the signal's noise current, in excess of shot noise. Hence APDs have found application in detection systems where the electrical noise introduced by following circuitry is greater than the noise introduced by a unity gain photodiode. These principally include detection systems which need to operate under low incident photon fluxes or with high bandwidths. In such systems an APD's multiplication can provide a desirable enhancement in the overall system sensitivity. Increasing an APD's operational gain only enhances a system's sensitivity whilst the APD's noise is less than the noise of the following circuitry. Hence the rate at which an APD's noise increases with increasing multiplication is a key performance parameter. The noise power (I_n^2) generated by an APD can be described by equation 1,

$$I_n^2 = 2q I_{pr} M^2 F BW \quad (1)$$

where q is the electron charge, I_{pr} the primary photocurrent, M the avalanche multiplication factor, F the excess noise factor and BW the bandwidth.

An APD's excess noise results from the stochastic nature of the impact ionisation process, which leads to fluctuations in the instantaneous multiplication as individual injected carriers undergo different levels of multiplication. The impact ionisation of electrons and holes is described by the ionisation coefficients $a(\xi)$ and $\beta(\xi)$ respectively, representing the mean number of impact ionisation events per unit length travelled, as a function of electric field ξ . These ionisation coefficients vary from material to material and their accurate determination is essential to support the assessment of a material's suitability for use in APD applications, as well as the modelling of an APD's noise. Equations 2 and 3 (McIntyre, 1966) describe how, under the local model of impact ionisation, an APD's excess noise factor is related to its operational multiplication and the ratio of the ionisation coefficients, k .

$$F_e = kM_e + (1-k) \left(2 - \frac{1}{M_e} \right) \text{ where } k = \beta/a \quad (2)$$

$$F_h = kM_h + (1-k) \left(2 - \frac{1}{M_h} \right) \text{ where } k = \beta/a \quad (3)$$

Here M_e and F_e are the average multiplication and excess noise initiated by a primary photocurrent consisting of only electrons, injected from the p-type side of the depletion region. Similarly M_h and F_h are the average multiplication and excess noise initiated by a primary photocurrent consisting of only holes, injected from the n-type side. The relationship between F , M and k defined by equations 2 and 3 is plotted in figure 1.

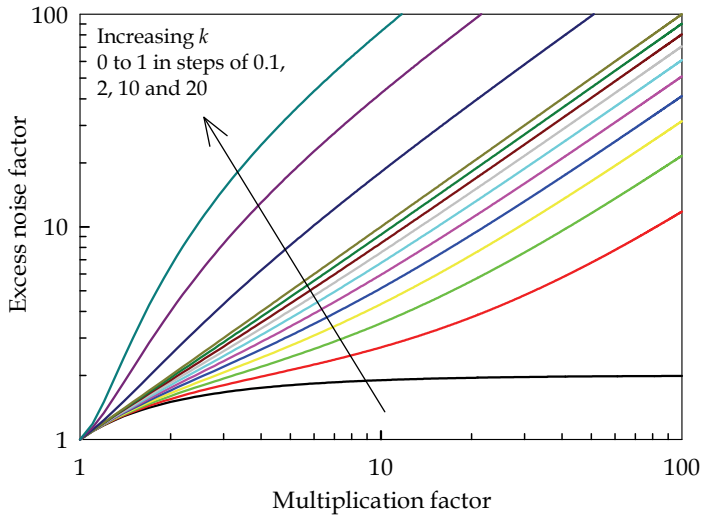


Fig. 1. The dependence of an APD's excess noise factor on its operational multiplication factor and the k of its multiplication medium, as defined by the local model (McIntyre, 1966).

Two important APD design principles can be taken from equations 2 and 3. Firstly, excess noise is always lower when only the carrier type with the highest ionisation coefficient is injected into the multiplication region, making $k \leq 1$. Secondly, in order to minimise the excess noise factor it is desirable to fabricate the multiplication region of an APD from a material with highly disparate ionisation coefficients, ideally one in which one of the ionisation coefficients is zero such that k also becomes zero.

The aggregate influence of an APD's multiplication and excess noise on the overall sensitivity of a light detecting system clearly varies depending on the system considered. To illustrate a typical case, figure 2 shows the sensitivity of a 10 Giga bit per second (Gbps) optical communications receiver, modelled as a function of its APD's multiplication and the k of the APD's gain medium. The APD's gain-bandwidth product limit is not considered in this illustrative case. From the results shown in figure 2 it can be seen that the lower the k of the APD's gain medium, the better the receiver sensitivity, and the higher the optimum APD gain in the absence of gain-bandwidth product limits. In the optimum case where $k = 0$, substantial improvements in receiver sensitivity are predicted as the APD's multiplication is increased. Furthermore it has been shown that both an APD's transit time limited bandwidth and its gain-bandwidth product limit increase as k reduces (Emmons, 1967).

The clear advantage afforded by employing materials with disparate ionisation coefficients in APDs, has led to a long term effort to characterise the ionisation coefficients in most common semiconductor materials (Stillman and Wolfe, 1977; Capasso, 1985; David and Tan,

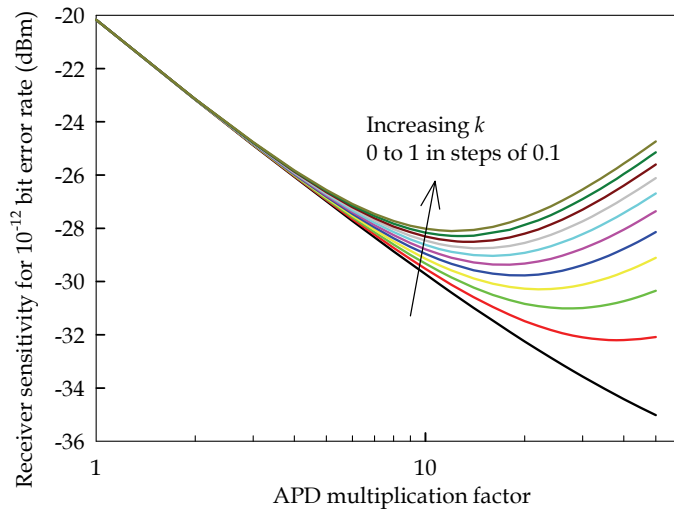


Fig. 2. The modelled receiver sensitivity of a 10 Gbps receiver as a function of its APD's operational multiplication factor and the k of its APD's gain medium.

2008). Until recently the optimum case, where $k = 0$, remained an unachievable theoretical ideal, with most materials exhibiting $0.1 < k < 1$. Indeed, unable to identify sufficiently capable materials, some researchers resorted to trying to engineer superlattice structures in which the ionisation coefficients were more disparate (Capasso *et al.*, 1982; Yuan *et al.*, 2000). Beck *et al.* were the first to report APD characteristics consistent with $k = 0$ in 2001, when they reported results from $\text{Hg}_{0.7}\text{Cd}_{0.3}\text{Te}$ APDs (Beck *et al.*, 2001). They have since shown that for a number of compositions β remains essentially zero in $\text{Hg}_{x-1}\text{Cd}_x\text{Te}$ APDs detecting in the short, mid and long wave infrared (SWIR, MWIR and LWIR) (Beck *et al.*, 2006). They coined the phrase electron-APD (e-APD) to describe such APDs where only electrons undergo impact ionisation. As desirable as some of the properties of $\text{Hg}_{x-1}\text{Cd}_x\text{Te}$ e-APDs undoubtedly are, $\text{Hg}_{x-1}\text{Cd}_x\text{Te}$ itself remains a challenging material to work with. It is not readily available through commercial foundries, unlike group IV and III-V materials, and is relatively expensive. It also becomes unstable at lower temperatures than other established semiconductors. Furthermore it can suffer from compositional non-uniformity issues over imaging array sized areas and in some cases cannot be as highly doped as III-V materials. Hence it remains desirable to identify a more widely available III-V material which exhibits comparable e-APD properties. Recent characterisation and development work on InAs APDs has shown that they can meet this desire for the first time (Marshall *et al.*, 2008; 2009; 2010).

This chapter presents the emerging InAs e-APD, summarising its properties using both recently published data and new results. It is shown that multiplication and excess noise in InAs APDs match those expected for the emerging e-APD subclass. Furthermore the specific and at times unique characteristics of electron avalanche multiplication in InAs are discussed. The ability to characterise InAs e-APDs and demonstrate their desirable properties has been underpinned by the development of new fabrication procedures, the key aspects of which are also discussed here. Finally the potential for deploying InAs e-APDs in several significant applications is discussed. All results presented here were

obtained from homojunction InAs $p-i-n$ and $n-i-p$ diode structures, grown by molecular beam epitaxy (MBE) or metal organic vapour phase epitaxy (MOVPE), in the EPSRC national centre for III-V technologies at The university of Sheffield, UK. The principle difference between the various structures characterised was the intrinsic region width. Hence whenever experimental results are presented here, the type of diode structure measured and its intrinsic region width are detailed. All device fabrication and characterisation work was undertaken within the Electronic and Electrical Engineering department at The University of Sheffield.

2. Avalanche multiplication and excess noise in InAs e-APDs

2.1 Avalanche multiplication

The magnitude of the impact ionisation coefficients a and β are usually determined through measurements of the photomultiplication factors M_e and M_h . It has been shown (Marshall *et al.*, 2010) that in InAs $p-i-n$ diodes significant electron initiated multiplication can be achieved whilst hole initiated multiplication in InAs $n-i-p$ diodes remains negligible across the same electric field range. The M_e measured on three $p-i-n$ diodes with a range of intrinsic widths and the M_h measured on a $n-i-p$ diode, are shown in figure 3a. The measurements were taken using a lock-in amplifier and phase sensitive detection of the photocurrent. This was generated by an appropriate laser wavelength such that all absorption took place within the doped p - and n -type cladding layers, allowing M_e to be measured on $p-i-n$ diodes and M_h to be measured on $n-i-p$ diodes. The results clearly show that $\beta \sim 0$ in InAs, within the electric field range exercised, also making $k \sim 0$. It should be noted that this finding is in contradiction to the only previously reported experimental study for avalanche multiplication in InAs. Mikhailova *et al.* reported that β was approximately 10 times greater than a in InAs, at 77K (Mikhailova *et al.*, 1976). This discrepancy is given more consideration in a number of journal papers (Marshall *et al.*, 2008; 2009; 2010); here it will simply be noted that during the new study of InAs e-APDs reviewed in this chapter, more than 20 different InAs diode structures have been characterised at room temperature, and all results are consistent with the finding that $\beta \sim 0$.

The most robust determination of the relative magnitude of a and β in any material comes from the measurement of M_e and M_h on a single diode structure, eliminating any uncertainty over variations in layer thickness and electric field profiles. In order to achieve this for InAs, the substrate was removed from a sample of fully fabricated $n-i-p$ diodes. This was achieved through a combination of mechanical thinning and selective wet etching. This made it possible to measure M_h by illuminating the top side of the diodes and M_e by illuminating the substrate side of the same diodes. The photomultiplication results taken in this way are shown in figure 3b and confirm that $a \gg \beta$ in InAs at room temperature, with $\beta \sim 0$, making it possible to realise the first III-V based e-APDs from InAs.

The avalanche multiplication characteristics measured on e-APDs differ from those of all conventional APDs. In conventional APDs not only does the injected carrier type (e.g. electrons) undergo impact ionisation when transiting the depletion region (from p - to n -type claddings), but secondary carriers of the other type (holes) generated by impact ionisation, also undergo impact ionisation themselves when transiting the depletion region in the opposite direction (towards the n -type cladding), generating yet more carriers of the injected type. One possible sequence of impact ionisation events in a conventional APD is shown schematically in figure 4. If the electric field within such an APD is increased, in turn

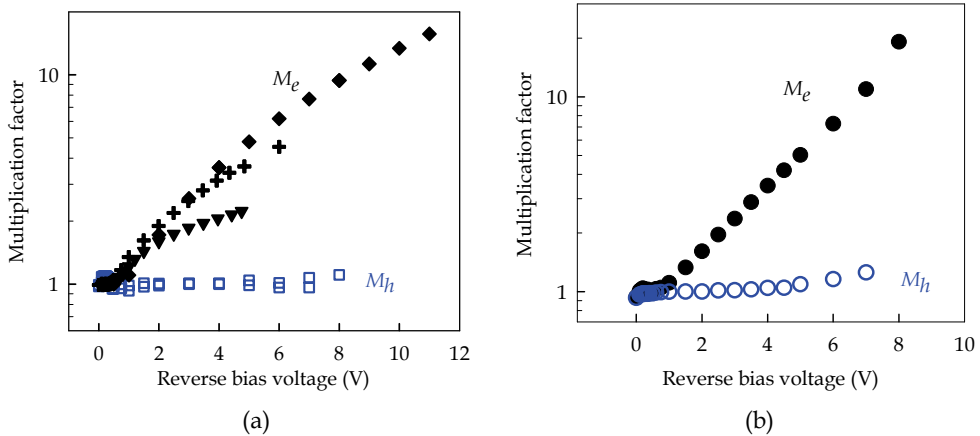


Fig. 3. Photomultiplication characteristics M_e and M_h for InAs diodes, measured on; (a) three $p-i-n$ diodes and one $n-i-p$ InAs diode, with intrinsic region widths of $3.5\mu\text{m}$ (\blacklozenge), $1.9\mu\text{m}$ (\blackplus), $0.8\mu\text{m}$ (\blacktriangledown) and $1.8\mu\text{m}$ (\square) respectively (Marshall *et al.*, 2010) (b) one $n-i-p$ diode with an intrinsic region width of $6\mu\text{m}$ doped at $\sim 7 \times 10^{14} \text{ cm}^{-3}$, with its substrate removed allowing both topside (\bullet) and substrate side (\circ) illumination.

increasing a and β , the avalanche multiplication can rise very rapidly due to the feedback in this avalanche. Indeed if the magnitude of a and β are sufficient that each carrier ionises on average at least once before leaving the depletion region, the multiplication factor becomes infinite and avalanche breakdown occurs.

By contrast in e-APDs the feedback provided by hole impact ionisation is absent. As a result the avalanche of electron impact ionisation events, from which the multiplication is solely derived, builds up in a single transit of the depletion region. Again one possible sequence of impact ionisation events within an e-APD is shown schematically in figure 4. This avalanche is more analogous with naturally occurring avalanches, where the material involved in the avalanche builds up as it falls in a single trip down a hill. The maximum number of impact ionisation events in an avalanche without feedback is limited since in practice neither a or the depletion width can become infinite. Hence true e-APDs never undergo an avalanche breakdown, instead exhibiting a progressively increasing multiplication as the bias voltage and commensurate electric field are increased. This is evident from the expression for multiplication in e-APDs under a constant electric field, given by equation 4 where w is the depletion width.

$$M_e = \exp(\alpha w) \tag{4}$$

Figure 5 compares the multiplication characteristics of some e-APDs with that of an InAlAs APD (Goh *et al.*, 2007), representative of conventional APDs. The multiplication factor minus one scale is used because it allows both the low and high gain characteristics to be presented clearly. There is essentially no discernible multiplication in the InAlAs APD below 7V, however once multiplication starts it rises quickly with increasing bias voltage and the APD breaks down at approximately 15V. In contrast multiplication is discernable in the e-APDs from lower voltages, in some cases less than 1V and it rises much more progressively with increasing bias voltage. On the logarithmic scale the rise in multiplication is approximately

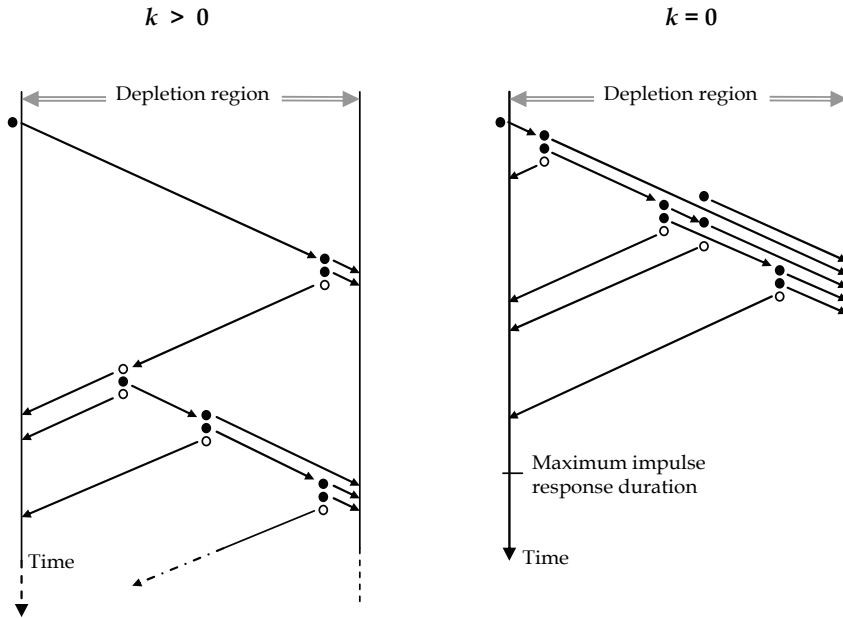


Fig. 4. Schematic representations of potential avalanches of impact ionisation events in multiplication regions where $k > 0$ and $k = 0$, showing the spatial and temporal distribution of impact ionisation by electrons (●) and holes (○).

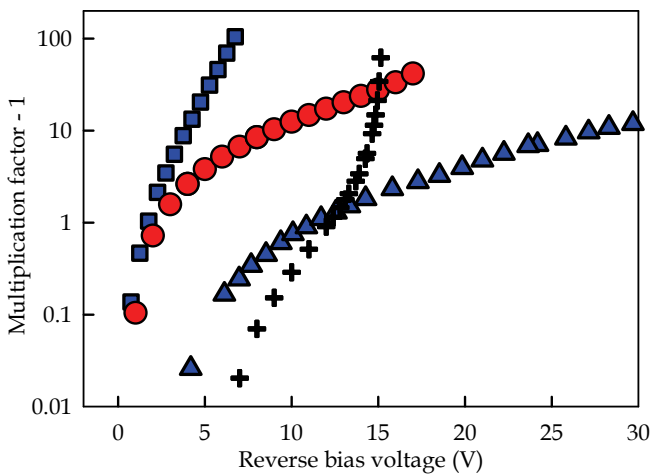


Fig. 5. A comparison between the M_e reported on APDs of different materials including, an InAs diode with a $3.5\mu\text{m}$ intrinsic width (●) (Marshall *et al.*, 2010), $\text{Hg}_{x-1}\text{Cd}_x\text{Te}$ diodes with cut-off wavelengths of $4.2\mu\text{m}$ (■) and $2.2\mu\text{m}$ (▲) (Beck *et al.*, 2006), and an InAlAs diode (✦) (Goh *et al.*, 2007).

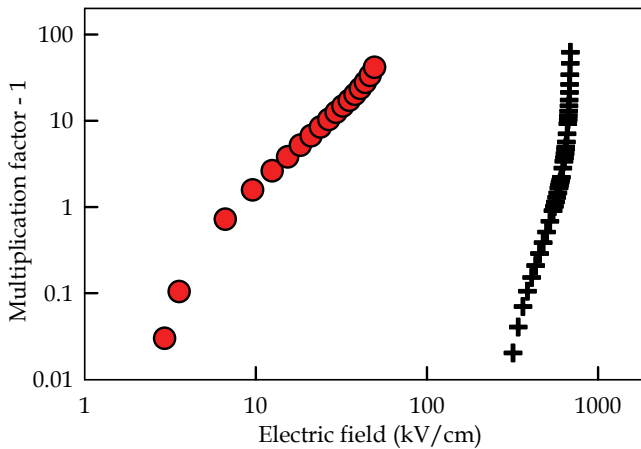


Fig. 6. A comparison between the M_e reported for an InAs diode with a $3.5\mu\text{m}$ intrinsic width (●) (Marshall *et al.*, 2010) and an InAlAs diode (✚) (Goh *et al.*, 2007), plotted against the electric field in the multiplication region.

linear after the initial turn on. As expected there is no breakdown observed in the e-APDs. A similar comparison against electric field is given in figure 6 and shows the same distinct characteristics, while also highlighting that avalanche multiplication in InAs e-APDs occurs at a much lower electric field than in conventional APDs.

It is worthwhile considering the bias dependence of the multiplication characteristics shown in figure 5, in relation to the concomitant biasing circuit requirements for each APD. Multiplication in all APDs is by nature dependent on the bias voltage applied to them; however it is undesirable for the multiplication to vary dramatically in response to small unintentional fluctuations in the nominal bias voltage. Conventional APDs need to be biased close to their breakdown voltage to provide significant multiplication, and hence are sensitive to bias voltage fluctuations. For example if the InAlAs APD reported in figure 5 were to be biased for a nominal multiplication of 10, a fluctuation of $\pm 0.25\text{V}$ about the nominal bias voltage would give rise to the actual multiplication varying between approximately 7 and 18. If a nominal gain of 100 were to be considered the variation in gain would be even more dramatic. By comparison if the InAs e-APD reported in figure 5 were to be biased for a nominal multiplication of 10, the same fluctuation of $\pm 0.25\text{V}$ about the nominal bias voltage would only result in the actual multiplication varying between approximately 9.5 and 10.6. Hence a further advantage of e-APDs, particularly when an APD needs to be operated at a high multiplication, is that their gain is less sensitive to fluctuations in their bias voltage.

2.2 Excess noise

The e-APD nature of InAs APDs has been further confirmed by excess noise measurements (Marshall *et al.*, 2009). The F_e measured on InAs *p-i-n* diodes, shown in figure 7, falls slightly below the local model prediction for $k = 0$ as given by equation 2. This excess noise is comparable to that reported for SWIR sensitive $\text{Hg}_{x-1}\text{Cd}_x\text{Te}$ e-ADPs, although it is somewhat higher than that reported for MWIR sensitive $\text{Hg}_{x-1}\text{Cd}_x\text{Te}$ e-APDs (Beck *et al.*, 2006). To allow comparison with the characteristic of a conventional APD, the excess noise measured

on an InAlAs APD is also shown in figure 7. As with all conventional APDs in which both carriers under go impact ionisation, the excess noise in the InAlAs APD rises with increasing multiplication. In comparison away from the lowest gains, the excess noise in the e-APDs does not continue to rise. This is clearly a desirable characteristic for APDs, as it improves the overall system sensitivity as shown earlier.

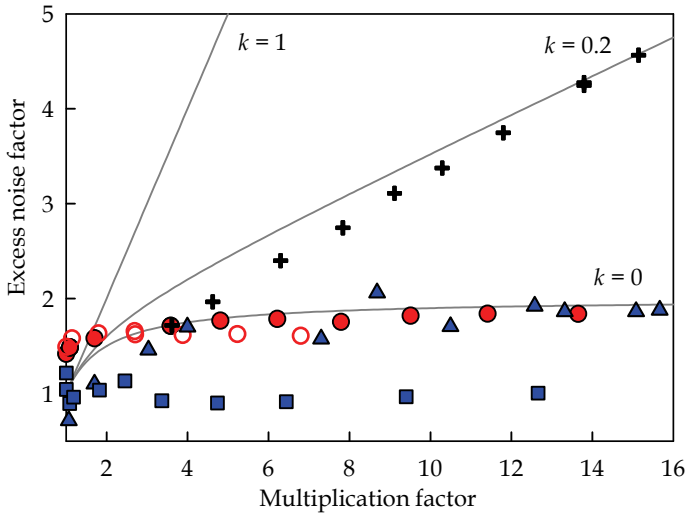


Fig. 7. A comparison between the F_e reported on APDs of different materials including, InAs diodes with a $3.5\mu\text{m}$ intrinsic width and radii of $50\mu\text{m}$ (●) and $100\mu\text{m}$ (○) (Marshall *et al.*, 2009), $\text{Hg}_{x-1}\text{Cd}_x\text{Te}$ diodes with cut-off wavelengths of $4.2\mu\text{m}$ (■) and $2.2\mu\text{m}$ (▲) (Beck *et al.*, 2006), and an InAlAs diode (✦) (Goh *et al.*, 2007).

In figure 7 it can be seen that the excess noise measured on the largest InAs APDs, for which the purest electron injection photocurrent was achieved, falls notably below the $k = 0$ local model prediction. To explain such excess noise below the lower limit case of the local model, it is necessary to consider the influence of deadspace, which is neglected from the local model. Deadspace has been described as the distance travelled by a carrier while it attains the ionisation threshold energy, or the distance travelled by a carrier while its energy rises into equilibrium with the electric field. Both descriptions attempt to address the reality that a carrier's ionisation probability does not become a non-zero function, described by its non-local ionisation coefficient, until it has travelled some distance. It is simplest to consider that it travels this distance with an ionisation probability of zero, leading to the first description. The effect of deadspace is to introduce determinism into both the spatial distribution of the impact ionisation events and the resulting multiplication experienced by individual carriers. This increased determinism leads to a reduction in the excess noise factor.

It is noted that deadspace is typically only considered to be of significance in conventional APDs with thin multiplication regions, less than a few hundred nanometres wide (Plimmer *et al.*, 2000). However it has been found that even in e-APDs with thick multiplication regions, such as the ones reported in figure 7, the deadspace can become significant with respect to the mean ionisation path length of electrons, a^{-1} , and hence noticeably affect the excess noise factor. When $k = 0$ the deadspace causes the excess noise factor to remain below

$F = 2$, reducing it towards the ultimate limit of $F = 1$. To achieve $F = 1$ it would be necessary for electrons to undergo impact ionisation immediately after transiting their deadspace, such that they transit the depletion region moving through a series of deadspaces between delta function ionisation probability density functions. The experimental results reported for $\text{Hg}_{0.3}\text{Cd}_{0.7}\text{Te}$ (Beck *et al.*, 2006) indicate that they are operating in approximately this ideal way.

2.3 Electron ionization coefficient

To allow modelling of the multiplication within arbitrary InAs e-APDs, an electron ionisation coefficient has been reported based on the multiplication results presented in figure 3 (Marshall *et al.*, 2010). This coefficient is parameterised as shown in equation 5.

$$\alpha = 4.62 \times 10^4 \exp \left[- \left(\frac{1.39 \times 10^5}{|\xi|} \right)^{0.378} \right] \text{ cm}^{-1} \tag{5}$$

The new room temperature electron ionisation coefficient for InAs is shown in figure 8 together with selected other electron ionisation coefficients. Amongst the materials in which impact ionisation has been well characterised, $\text{In}_{0.53}\text{Ga}_{0.47}\text{As}$ is considered to have an atypically high electron ionisation coefficient at low electric fields (Ng *et al.*, 2003). In comparison significant electron ionisation occurs in InAs from much lower electric fields. Indeed the maximum electric field for which a has been calculated in InAs is lower than the minimum electric field for which a could be determined in $\text{In}_{0.53}\text{Ga}_{0.47}\text{As}$. This greatly enhanced electron impact ionisation at low electric fields is of pivotal importance for InAs APDs. It is considered to be both the reason that meaningful avalanche multiplication can be achieved at all in practical devices and the reason that they operate as e-APDs.

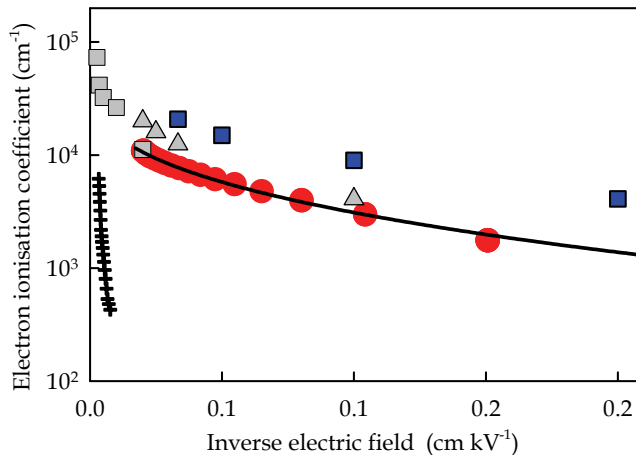


Fig. 8. A comparison between the electron ionization coefficients reported for different materials including, InAs as calculated from experimental results (●) (Marshall *et al.*, 2010), as parameterised (line) and as modelled by both Bude and Hess (1992) (■) and Brennan and Mansour (1991) (▲), $\text{Hg}_{0.3}\text{Cd}_{0.7}\text{Te}$ as modelled by Brennan and Mansour (1991) (■) and $\text{In}_{0.53}\text{Ga}_{0.47}\text{As}$ as calculated from experimental results by Ng *et al.* (2003) (✚).

$\text{In}_{0.53}\text{Ga}_{0.47}\text{As}$ has not been used as the gain medium of APDs because it generally suffers from excessive tunnelling current before the electric field becomes high enough for significant multiplication to be obtained. InAs has a significantly smaller bandgap and commensurately higher tunnelling current at a given electric field, however because a is high enough at low electric fields, practical APDs can still be realised without excessive tunnelling current. Furthermore InAs APDs operate as e-APDs, whereas other III-V based APDs do not, due the atypically enhanced a within their operational electric field range, rather than an atypically suppressed β . Indeed it is expected that could InAs be characterised at higher electric fields, hole impact ionisation would be found to commence somewhat below the electric field required for hole impact ionisation in $\text{In}_{0.53}\text{Ga}_{0.47}\text{As}$, $\sim 150 \text{ kVcm}^{-1}$. However the tunnelling current at such electric fields is likely to make characterisation impossible.

As shown in figure 8, $\text{Hg}_{0.3}\text{Cd}_{0.7}\text{Te}$ is modelled to exhibit an even higher a than InAs, which is consistent with the higher gain and lower noise reported, as shown in the comparisons in figures 5 and 7 respectively. Brennan and Mansour (1991) and Bude and Hess (1992) both modelled a in InAs and reported results broadly in line with the new experimentally derived a . Brennan and Mansour suggested a should be slightly higher at 77K than the newly derived room temperature a . Working purely theoretically Bude and Hess modelled a for a higher electric field range than it has so far been possible to exercise in practice, however their lowest data point aligns with the new a well.

The combination of a being only weakly dependent on electric field and β being approximately zero, results in a final atypical characteristic of InAs e-APDs. This trend can be observed in the M_e results shown in figure 3 and should be explained since it has significant implications for the design of InAs e-APDs. Usually when the multiplication characteristics measured on $p-i-n$ diodes with different intrinsic widths are compared as a function of the applied voltage, the multiplication at any given voltage is highest in the diode with the thinnest depletion width. However in InAs $p-i-n$ diodes this trend is not seen, instead the highest multiplication at any given voltage is achieved in the diode with the widest intrinsic region and hence also the widest depletion region and lowest electric field. Uniquely in InAs e-APDs an increase in the depletion width over which the unidirectional electron avalanche can build up, has a greater influence on the APD's multiplication factor than the concomitant reduction in a due to the lower electric field. This unique trend can be exploited to improve the characteristics of InAs e-APDs, unimpeded by some of the classical APD design trade-offs. Increasing the depletion width in an InAs e-APD increases the multiplication achieved at low bias voltages, making it easier to integrate the APD into a system. Furthermore it also leads to a reduction in the electric field within the APD, improving its reliability and reducing tunnelling current. As a result of this it is desirable for almost all applications, that the intrinsic width in InAs e-APDs is increased as much as practical, since this results in demonstrably better device performance parameters.

3. The fabrication of practical InAs e-APDs

It was only possible to successfully undertake the characterisation of InAs e-APDs reported in the previous section, following the development of a growth and fabrication process which was capable of producing InAs diodes with reduced and controlled reverse leakage current. Minimising the reverse leakage current in InAs diodes is particularly challenging

due to the low bandgap energy of InAs and its predisposition towards forming low impedance surfaces (Noguchi *et al.*, 1991).

Efforts to reduce the reverse leakage current in InAs APDs started with development of the epilayer growth conditions. The InAs used in this work was grown by MBE and MOVPE on *p*-type InAs substrates. Following a RHEED monitored clean-up at 500°C, MBE growth was performed at ~0.8 monolayers per a second with a substrate temperature of 470°C. MOVPE growth commenced with a 620°C substrate clean-up, followed by growth at ~10 Å/s with a substrate temperature of 600°C. During all growths the two key aims were to:

- Minimise the defect density so as to minimise the bulk leakage current and increase the maximum bias voltage which could be applied without the diodes failing.
- Minimise the background doping concentration in the intrinsic region, so that the depletion width and hence also the multiplication, was maximised.

Minimising the background doping was found to be easier using MBE, with background doping densities $\leq 1 \times 10^{15} \text{ cm}^{-3}$ routinely achievable and a minimum electrically active doping density of $\sim 2 \times 10^{14} \text{ cm}^{-3}$ measured. However maintaining the crystal quality during the growth of diode structures $> 5 \mu\text{m}$ thick was challenging and ultimately MOVPE was found to be the preferred technique for growing the thickest InAs diode structures. The higher growth rate made it reasonably practical to grow total epitaxial thicknesses of $10 \mu\text{m}$. Furthermore the MOVPE grown InAs was also found to be electrically more robust than MBE grown InAs. MOVPE grown diodes were less prone to non ideal increases in bulk leakage under higher bias voltages and were able to withstand higher maximum voltages without failing. Keeping the background doping down to acceptable levels was more of an issue than with MBE, however following optimisation work it was possible to obtain doping densities slightly below $1 \times 10^{15} \text{ cm}^{-3}$.

Fabricating InAs mesa diodes with low leakage currents is arguably more challenging than growing good quality InAs epilayers. The principle issue is the predisposition of etched InAs surfaces to become low impedance. Such surfaces link the *p*- and *n*-type regions of the mesa diode with a low resistance sidewall, down which significant surface leakage current can readily flow. Wet chemical etching typically produces mesa sidewalls with less damage than dry etch etching does, and for InAs e-APD fabrication wet etchants were again found to be preferable. A number of etchants were tested during this work (Marshall *et al.*, 2007) and the optimum etching routine developed was as detailed below.

1. Etch the mesa to approximately $0.5 \mu\text{m}$ less than the desired total depth in a 1 : 1 : 1 mixture of H_3PO_4 : H_2O_2 : H_2O
2. Etch the mesa for 30 seconds in a 1 : 8 : 80 mixture of H_2SO_4 : H_2O_2 : H_2O .
3. Remove the resist from the sample using acetone only
4. Dip the unmasked sample in the 1 : 1 : 1 mixture of H_3PO_4 : H_2O_2 : H_2O for 10 seconds, quench in deionised water and then immediately dip the sample in the 1 : 8 : 80 mixture of H_2SO_4 : H_2O_2 : H_2O for 20 seconds
5. Avoid further immersion of the mesa sidewall

The sequential use of the two etchants consistently produces a better result than using either of them individually. It is postulated that the first etchant has a tendency to leave an indium rich surface whereas the second has a tendency to leave an arsenic rich surface. Using them sequential with the appropriate etch durations may produce a balanced InAs surface. Returning the sample to the etchants after the mask has been removed results in all exposed InAs surfaces being etched slightly. Whilst this is generally not desirable it is possible to

design a fabrication process and diode structure which can tolerate it and the procedure does produce diodes with consistently lower surface leakage current.

As with many aspects of InAs diode fabrication, there is little information in the literature regarding the formation of ohmic contacts with InAs. However in this respect the surface properties of InAs are favourable and for the majority of this work Ti / Au contacts, 20nm / 200nm thick, were found to be adequate for both *n*- and *p*-type contacts. Indeed using this metallisation the typical contact resistance was in the order of 10Ω.

Using the optimised etching routine it was possible to fabricate InAs e-APDs with negligible surface leakage current across a wide range of bias voltages. Figure 9 shows the reverse leakage current characteristics measured on InAs mesa diodes with four different radii, along with the current densities calculated for the different diodes. The excellent consistency between the current densities calculated for the diodes with different areas, indicates that the surface leakage current was negligible in all diodes. If etched incorrectly the leakage current in diodes like these can reach 10mA at a reverse bias voltage as low as 1V or less.

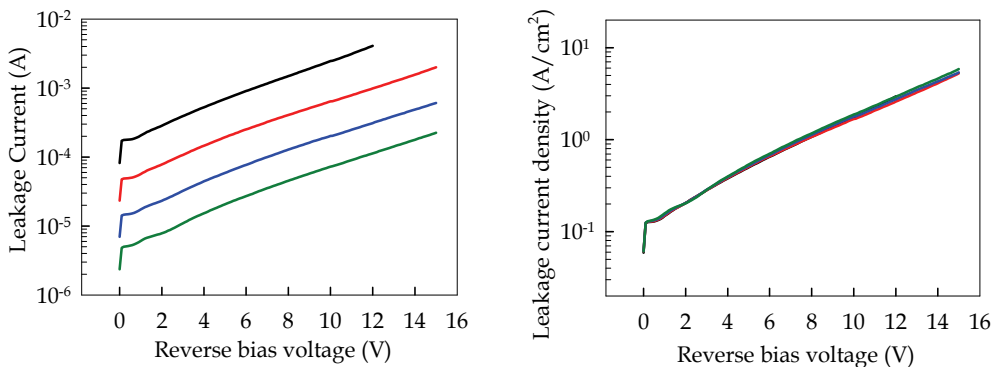


Fig. 9. The reverse leakage current measured on InAs *n-i-p* diodes with 200μm (black), 100μm (red), 50μm (blue) and 25μm (green) radii and intrinsic region widths of 6μm doped at $\sim 1 \times 10^{15} \text{ cm}^{-3}$, together with the commensurate leakage current density calculated.

The leakage characteristics of InAs photodiodes are rarely reported beyond a reverse bias of 0.5V, because to date they have been exclusively used as unity gain detectors. Not only does the leakage current in the InAs e-APDs developed during this work remain controlled under previously unreported high bias voltages, but it also compares favourably with reported unity gain InAs photodiodes at low bias voltages. Figure 10 shows a comparison of the leakage current densities in a number of InAs photodiodes. Under low bias voltages the lowest leakage current is observed in an MBE grown *p-i-n* diode. This diode structure includes a lattice matched AlAsSb layer immediately under the *p*-type contact, designed to block the diffusion of minority electrons from the surface or contact (Marshall *et al.*, 2007). Diodes with this blocking layer routinely yielded the lowest leakage currents at low reverse bias voltages. The MOVPE grown *n-i-p* diode exhibits only slightly higher leakage at low reverse bias, remaining below the level reported by others for InAs diodes. Under higher bias voltages this diode exhibits the lowest leakage current, typical of MOVPE grown diodes.

4. The potential for exploiting InAs e-APDs

4.1 Leakage current

The new InAs e-APD technology offers a III-V based alternative to the high performance but exotic $\text{Hg}_{x-1}\text{Cd}_x\text{Te}$ e-APD technology. The core multiplication and excess noise characteristics of these new APDs are undoubtedly desirable for a number of applications, however to assess their true suitability the most important parameter to consider is the leakage current. Due to their narrow bandgap, InAs APDs will inevitably exhibit higher leakage than similar APDs fabricated from wider bandgap materials. Whether or not this leakage can be tolerated, or suppressed through cooling, ultimately depends upon the specific application of interest. Based on the characterisation and development work carried out to date it is possible to make some observations and predictions regarding leakage current in InAs e-APDs, so as to support assessment of their potential. The leakage currents which affect InAs e-APDs under low and high bias voltages are considered separately. It has already been shown that surface leakage current can be adequately suppressed at room temperature, and with further development it is likely that the same can be achieved at lower temperatures. Hence surface leakage is not included in this consideration of the unavoidable mechanisms contributing to the leakage current in InAs e-APDs.

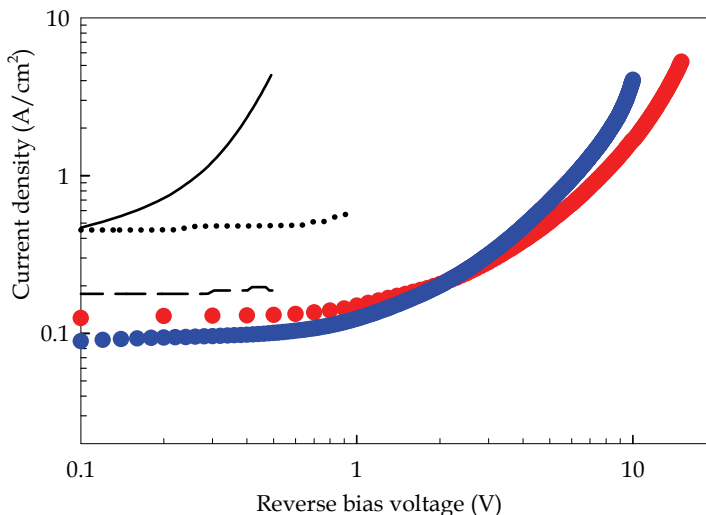


Fig. 10. A comparison between the reverse bias leakage characteristics measured on two of the new InAs e-APDs and those reported for or measured on other InAs diodes including, a commercial diode (solid line), a planar diode (Iwamura and Watanabe, 2000) (dotted line) and the best prior mesa diode (Lin *et al.*, 1997) (dashed line). The two InAs diodes were a p - i - n diode with a $3.5\mu\text{m}$ intrinsic width (\bullet) and a n - i - p diode with an intrinsic region width of $6\mu\text{m}$ doped at $\sim 1 \times 10^{15} \text{cm}^{-3}$ (\bullet).

At room temperature and low reverse bias the leakage current in InAs e-APDs is dominated by bulk diffusion current. The two InAs e-APDs reported in figure 10 show a low bias leakage current density of $\sim 100 \text{mAcm}^{-2}$. This level is typical of the InAs e-APD technology at present; however lower leakage current densities have been measured, down to \sim

30mA/cm². It is considered that there remains considerable scope for reducing the defect density in the epitaxial InAs through further development of the epitaxial growth conditions, and hence it is likely that this leakage current density can be reduced further. Beyond improving the crystal quality, the devices will need to be cooled to suppress the leakage current density even more. As the temperature is reduced it is typical for the leakage to change from being diffusion dominated to generation and recombination dominated (Krier *et al.*, 1998). At this time it is not known at which temperature this transition will occur for the new InAs e-APDs. Figure 11 provides an estimate of the upper and lower limits within which the leakage current density is likely to fall, as the temperature is reduced. The upper and lower limits were calculated based on the measured room temperature leakage current density falling in line with generation and recombination and diffusion current theory respectively, using the published temperature dependence of the intrinsic carrier concentration in InAs (Rogalski, 1989; Mikhailova, 1996). It is expected that initially as the temperature is reduced the leakage current will remain diffusion dominated and follow the lower of the lines, before changing to become generation and recombination dominated and fall further with the gradient of the higher line.

As the reverse bias voltage is increased to multiply the photocurrent, the leakage current also undergoes multiplication. In practice it has been found that the leakage current usually increases at approximately the rate of M_e . There is considered to be little scope for reducing this. Hence to obtain an estimate of the leakage current in an InAs e-APD of arbitrary size, operating at an arbitrary gain, the likely low bias leakage current density can be multiplied by the APD's area and the desired gain.

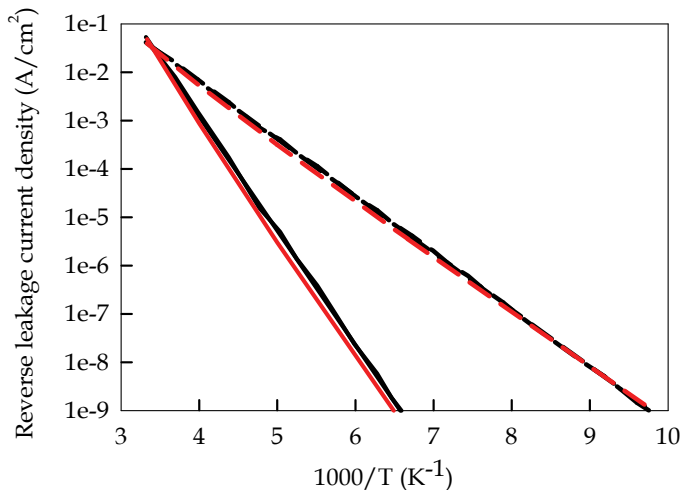


Fig. 11. Predicted boundary limits for the temperature dependant reverse leakage current density in InAs APDs under a low 0.25V reverse bias. Extrapolated from a room temperature result using published intrinsic carrier concentrations (Rogalski, 1989) (red lines) (Mikhailova, 1996) (black lines), considering diffusion limited leakage (solid lines) and G&R limited leakage (dashed lines) and excluding surface leakage.

The final leakage current related concern for APDs made from narrow bandgap materials is tunnelling current. InAs has both a low electron effective mass and a narrow bandgap, which combine to give significant band-to-band tunnelling current at much lower electric fields than in other materials used in established APDs. As identified earlier in this chapter, the deleterious effect of this is mitigated by a being significantly higher at low electric fields than in established APD materials. As a result it has been possible to fabricate many InAs e-APDs in which significant multiplication can be achieved while tunnelling current remains negligible. To illustrate this figure 12 shows the multiplication and leakage current density measured on one such e-APD, together with the band-to-band tunnelling current density expected from its structure. In practice it is considered that an intrinsic region width of $> 3\mu\text{m}$ with a background doping concentration $\leq 1 \times 10^{15} \text{ cm}^{-3}$, will be sufficient to avoid tunnelling current affecting most applications.

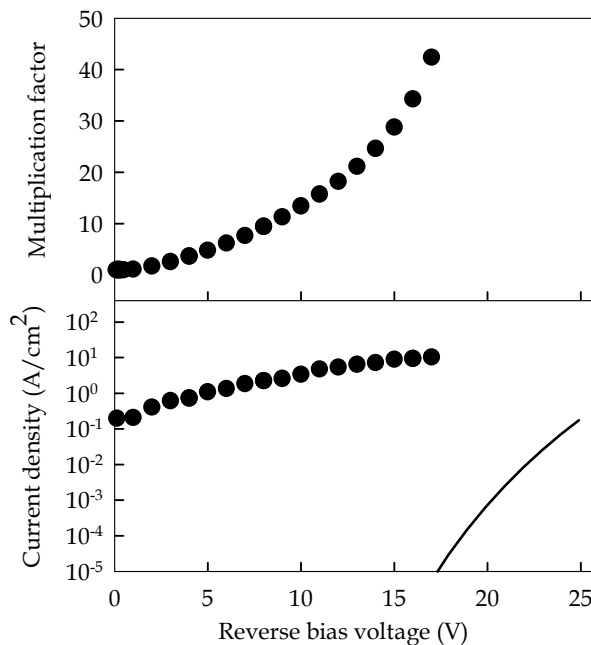


Fig. 12. The multiplication factor and reverse leakage current density measured on an InAs *p-i-n* diode with a $3.5\mu\text{m}$ intrinsic region width, together with the expected tunnelling current density for the structure, shown against reverse bias voltage.

4.2 Potential applications

InAs e-APDs will probably find application in systems where their extended spectral response, lower excess noise and increased bandwidth in the presence of gain, offer a clear advantage. Where this is not the case, the level of leakage current commensurate with the narrow bandgap of InAs and the increased cost per unit area are likely to make them

unattractive, compared to existing detector options. Below are some of the applications which are likely to suit the unique characteristics of InAs e-APDs.

Imaging arrays and LIDAR

InAs e-APD arrays could be used for passive imaging across the full SWIR range, offering extended spectral sensitivity over InGaAs arrays. However since their response only reaches the bottom of the MWIR window, their advantage in such passive applications would be limited. More promising applications lie in the area of active imaging or LIDAR (light detection and ranging), where $\text{Hg}_{x-1}\text{Cd}_x\text{Te}$ e-APDs have already started to find applications (Baker *et al.*, 2004; Beck *et al.*, 2007). Currently such systems operate at a wavelength of $1.55\mu\text{m}$ due to the availability of cheap sources and InAs e-APDs can also offer high responsivity at this wavelength. Valuably InAs e-APDs could also support the use of longer SWIR wavelengths which would not be detectable with standard InGaAs detectors, affording a degree of covertness when desired. Thermoelectric cooling is likely to be required in such applications.

When APDs are used in array applications, gain uniformity across the array is an important consideration and in this respect InAs e-APDs can provide an advantage compared other APD options. Firstly, the InAs back-plane can be highly doped to reduce voltage drops across the array area. Secondly, InAs does not suffer from the compositional non-uniformity that $\text{Hg}_{x-1}\text{Cd}_x\text{Te}$ or other ternary alloys can exhibit, and hence all APDs on the array should have near identical voltage dependent gain characteristics. Furthermore should the bias voltage vary slightly across the array, the gain at individual pixels will vary much less significantly than it would for non e-APD technologies as highlighted in section 2.1.

Gas detection or monitoring

Many important gases have absorption lines in the spectral range between visible and $3.5\mu\text{m}$ wavelengths, over which InAs e-APDs are sensitive, these include CO_2 at $2.05\mu\text{m}$. Optimum applications for InAs e-APDs are likely to be those which require the profiling of gas concentrations across a significant distance. In such applications the ability of InAs e-APDs to greatly amplify weak signals will be advantageous, as will their ability to maintain a high bandwidths when operating at high gains, something which conventional APDs cannot do.

Optical communications

InAs e-APDs may appear to be an unlikely choice for high bit rate optical communication systems, due to their wide depletion regions. In conventional materials such wide depletion regions would result in the APD having an unacceptably low transit time limited bandwidth. However because there is no feedback within the avalanche multiplication in InAs e-APDs, their maximum impulse response duration (t_{max}) is the sum of the transit times for electrons and holes, irrespective of operational gain. In terms of the depletion width (w) and the average velocities of electrons (v_e) and holes (v_h), this is given by equation 6. Using the electron saturated drift velocity calculated by satyandah *et al.* (2002) and the hole saturated drift velocity for InGaAs, it is possible to estimate this maximum impulse response duration to be only ~ 60 ps, for an InAs e-APD with a $3\mu\text{m}$ wide intrinsic region. The high speed potential of InAs e-APDs is further assisted by the low capacitance associated with the wide depletion region and the very low cladding and contact resistances

which are achievable. These combine to make RC bandwidth limiting less of a concern than in established APD technologies.

$$t_{\max} = \frac{w}{v_e} + \frac{w}{v_h} \quad (6)$$

Because InAs e-APDs are likely to require some thermoelectric cooling to meet the leakage current targets for communications applications, it is unlikely that InAs e-APDs would be considered as an alternative for the established InAlAs/InGaAs APDs in high volume applications. However they may find selective application in systems where high gain and the maximum possible sensitivity are required, without a drop in the available bandwidth. Free space optical links are considered a potential application, since unimpeded by a classical gain-bandwidth product limit, InAs e-APDs could provide a greatly enhanced sensitivity dynamic range. This would allow the link to be maintained in bad weather by increasing the APD gain freely as required.

5. Conclusion

In this chapter the emerging InAs e-APD has been introduced. Experimental results have been presented, which confirm that it exhibits the fundamental characteristic of an e-APD, namely that only electrons undergo appreciable multiplication within it. The key advantage of e-APDs, their reduced excess noise, has been demonstrated and the potential benefit this affords a system has been introduced. Furthermore many of the unique characteristics of InAs e-APDs have been discussed in detail. Hence this work provides an up to date summary of the fundamental properties of InAs e-APDs. It is noted that further fundamental characterisation would be desirable, particularly assessing the temperature dependence of the multiplication and leakage characteristics. Detailed physical modelling of the impact ionisation in e-APDs would also be desirable, to improve understanding of the physical processes involved.

Beyond the fundamental characterisation results, some of the fabrication processes which have enabled the realisation of practical InAs e-APDs, have also been presented. The leakage current to be expected in such devices has been discussed. Importantly it has also been shown that high gain APDs can be designed and fabricated to operate with negligible tunnelling current, despite the narrow bandgap of InAs.

The realisation of APDs in InAs has brought the ideal avalanche multiplication and excess noise characteristics of e-APDs into the readily available III-V material system for the first time. This brings with it the potential for more wide spread application of e-APDs, previously only achievable in the less readily available $\text{Hg}_{x-1}\text{Cd}_x\text{Te}$ system. Some of the applications where InAs e-APDs may offer an advantage have been highlighted, as have the specific characteristics which make them ideally suited to such applications.

6. Acknowledgements

The work reported here was carried out in the Electronic and Electrical Engineering department at the at the University of Sheffield, UK, within the research group of Dr. Chee

Hing Tan and Prof. John David, whom the author thanks most sincerely for securing the necessary funding and helping to direct the work.

The author also thanks Dr. Mathew Steer and Dr. Andrey Krysa for their expert MBE and MOVPE growth.

This work was substantially funded by the Electro-Magnetic Remote Sensing (EMRS) Defence Technology Centre, established by the UK Ministry of Defence and run by a consortium of SELEX Sensors and Airborne Systems, Thales Defence, Roke Manor Research and Filtronic.

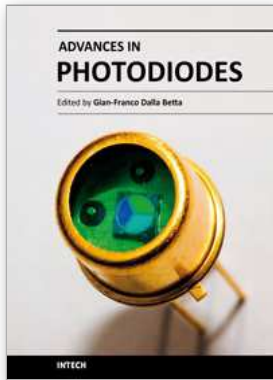
Patent no. GB0723858.7

7. References

- Baker, I., Duncan, S., & Copley, J. (2004). A low noise laser-gated imaging system for long range target identification, *Proceedings of SPIE Vol. 5406 Infrared Technology and Applications*, pp. 133-144, Orlando, April 2004, SPIE, Bellingham
- Beck, J.D., Wan, C-F., Kinch, M.A., Robinson, J.E. (2001). MWIR HgCdTe avalanche photodiodes, *Proceedings of SPIE Vol. 4454 Materials for Infrared Detectors*, pp. 188-197, Orlando, April 2001, SPIE, Bellingham
- Beck, J., Wan, C., Kinch, M., Robinson, J., Mitra, P., Scritchfield, R., Ma, F. & Campbell, J. (2006). The HgCdTe electron avalanche photodiode, *J. Electronic Materials*, vol. 35, no. 6, (2006) 1166-1173
- Beck, J., Woodall, M., Scritchfield, R., Ohlson, M., Wood, L., Mitra, P. Robinson, J. (2007). Gated IR imaging with 128x128 HgCdTe Electron avalanche photodiode FPA, *Proceedings of SPIE Vol. 6542 Infrared Technology and Applications*, pp. 654217, Orlando, April 2007, SPIE, Bellingham
- Brennan, K.F. & Mansour, N.S. (1991). Monte Carlo calculation of electron impact ionization in bulk InAs and HgCdTe, *J. Appl. Phys.*, vol. 69, no. 11, (June 1991) 7844-7847
- Bude, J. & Hess, K. (1992). Thresholds of impact ionization in semiconductors, *J. Appl. Phys.*, vol. 72, no. 8, (October 1992) 3554-3561
- Capasso, F., Tsang, W.T., Hutchinson, A.L. & Williams, G. F. (1982). Enhancement of electron impact ionization in a superlattice: A new avalanche photodiode with a large ionization rate ratio, *Appl. Phys. Lett.*, vol. 40, no. 1, (January 1982) 38-40
- Capasso, F. (1985). Physics of avalanche photodiodes, in *Semiconductors and Semimetals - Lightwave Communications Technology*, vol. 22-D, Ed. W. T. Tsang, 1-172, Academic Press Inc., Orlando
- David, J.P.R. & Tan, C.H. (2008). Material considerations for avalanche photodiodes, *IEEE J. Sel. Top. Quantum Electron.*, vol. 14, no. 4, (July 2008) 998-1009
- Emmons, R.B. (1967). Avalanche-photodiode frequency response, *J. App. Phys.*, vol. 38, no. 9, (August 1967) 3705-3714
- Goh, Y.L., Marshall, A.R.J., Massey, D.J., Ng, J.S., Tan, C.H., Hopkinson, M., David, J.P.R., Jones, S.K., Button, C.C. & Pinches, S.M. (2007). Excess avalanche noise in $\text{In}_{0.52}\text{Al}_{0.48}\text{As}$, *IEEE J. Quantum Electron.*, vol. 43, no. 6, (June 2007) 503-507

- Iwamura, Y., Watanabe, N. (2000). InAs planar diode fabricated by Zn diffusion, *Japanese J. Appl. Phys.*, vol. 39, (2000) 5740-5745
- Krier, A., Gao, H.H., & Mao, Y. (1998). A room temperature photovoltaic detector for the mid-infrared (1.8-3.4 μ m) wavelength region, *Semicond. Sci. Technol.*, vol. 13, (1998) 950-956
- Lin, R-M., Tang, S-F., Lee, S-C., Kuan, C-H., Chen, G-S., Sun, T-P. & Wu, J-C. (1997). Room temperature unpassivated InAs p-i-n photodetectors grown by molecular beam epitaxy, *IEEE Trans. Electron Dev.*, vol. 44, no. 2, (February 1997) 209-213
- Marshall, A.R.J., Tan, C.H., David, J.P.R., Ng, J.S. & Hopkinson, M. (2007). Fabrication of InAs photodiodes with reduced surface leakage current, *Proceedings of SPIE Vol. 6740 Defence and Security Europe*, pp. 67400H, Florence, September 2007, SPIE, Bellingham
- Marshall, A.R.J., Tan, C.H., Steer, M.J. & David, J.P.R. (2008) Electron dominated impact ionization and avalanche gain in InAs photodiodes, *Appl. Phys. Lett.* vol. 93, no. 11, (September 2008) 111107
- Marshall, A.R.J., Tan, C.H., Steer, M.J. & David, J.P.R. (2009). Extremely low excess noise in InAs electron avalanche photodiodes," *IEEE Photon. Technol. Lett.*, vol. 21, no. 13, (July 2009) 866-868
- Marshall, A.R.J., Tan, C.H. & David, J.P.R. (2010). Impact Ionization in InAs Electron Avalanche Photodiodes, *IEEE Trans. Electron. Dev.*, vol. 57, no. 10, (October 2010) 2631-2638
- McIntyre, R.J. (1996). Multiplication noise in uniform avalanche diodes, *IEEE Trans. Electron Devices*, vol. ED-13, (January 1966) 164-168
- Mikhailova, M.P., Smirnova, M.M. & Slobodchikov, S.V. (1976) Carrier multiplication in InAs and InGaAs p-n junctions and their ionization coefficients", *Sov. Phys. Semicond.*, vol. 10, no. 5, (May 1976) 509-513
- Mikhailova, M.P. (1996). in Handbook Series on Semiconductor Parameters, vol.1, Eds. Levinshtein, M., Rumyantsev, S. & Shur, M., World Scientific, London
- Ng J.S., Tan, C.H., David, J.P.R., Hill, G. & Rees, G.J. (2003). Field dependence of impact ionization coefficients in In_{0.53}Ga_{0.47}As," *IEEE Trans. Electron Devices*, vol. 50, no. 4, (2003) 901-905
- Noguchi, M., Hirakawa, K. & Ikoma, T. (1991). Intrinsic electron accumulation layers on reconstructed clean InAs (100) surfaces, *Phys. Rev. Lett.*, vol. 66, no. 17, (April 1991) 2243-2246
- Plimmer, S.A., David, J.P.R. & Ong, D.S. (2000). The merits and limitations of local impact ionisation theory, *IEEE Trans. Electron Device.*, vol. 47, no. 5, (May 2000) 1080-1088
- Rogalski, A. (1989). InAs_{1-x}Sb_x infrared detectors, *Progress in Quantum Electronics*, vol.13, (1989) 191-231
- Satyanadh, G., Joshi, R.P., Abedin, N. and Singh. U. (2002). Monte Carlo calculation of electron drift characteristics and avalanche noise in bulk InAs," *J. Appl. Phys.*, vol. 91, no. 3, (February 2002) 1331-1338
- Stillman, G.E. & Wolfe, C.M. (1977). Avalanche Photodiodes, *Semiconductors and Semimetals*, Eds. Willardson, R.K. & Beer, A.C. vol.12, 291-393, Academic press, Orlando

Yuan, P., Wang, S., Sun, X., Zheng, X.G., Holmes, A.L. & Campbell, J.C. (2000). Avalanche photodiodes with an impact-ionization-engineered multiplication region, *IEEE Photon. Technol. Lett.*, vol. 12, no. 10, (October 2000) 1370-1372



Advances in Photodiodes

Edited by Prof. Gian Franco Dalla Betta

ISBN 978-953-307-163-3

Hard cover, 466 pages

Publisher InTech

Published online 22, March, 2011

Published in print edition March, 2011

Photodiodes, the simplest but most versatile optoelectronic devices, are currently used in a variety of applications, including vision systems, optical interconnects, optical storage systems, photometry, particle physics, medical imaging, etc. *Advances in Photodiodes* addresses the state-of-the-art, latest developments and new trends in the field, covering theoretical aspects, design and simulation issues, processing techniques, experimental results, and applications. Written by internationally renowned experts, with contributions from universities, research institutes and industries, the book is a valuable reference tool for students, scientists, engineers, and researchers.

How to reference

In order to correctly reference this scholarly work, feel free to copy and paste the following:

Andrew R. J. Marshall (2011). The InAs Electron Avalanche Photodiode, *Advances in Photodiodes*, Prof. Gian Franco Dalla Betta (Ed.), ISBN: 978-953-307-163-3, InTech, Available from:
<http://www.intechopen.com/books/advances-in-photodiodes/the-inas-electron-avalanche-photodiode>

INTECH

open science | open minds

InTech Europe

University Campus STeP Ri
Slavka Krautzeka 83/A
51000 Rijeka, Croatia
Phone: +385 (51) 770 447
Fax: +385 (51) 686 166
www.intechopen.com

InTech China

Unit 405, Office Block, Hotel Equatorial Shanghai
No.65, Yan An Road (West), Shanghai, 200040, China
中国上海市延安西路65号上海国际贵都大饭店办公楼405单元
Phone: +86-21-62489820
Fax: +86-21-62489821

© 2011 The Author(s). Licensee IntechOpen. This chapter is distributed under the terms of the [Creative Commons Attribution-NonCommercial-ShareAlike-3.0 License](#), which permits use, distribution and reproduction for non-commercial purposes, provided the original is properly cited and derivative works building on this content are distributed under the same license.